# The homogeneous nucleation of nonane

G. W. Adams, J. L. Schmitt, and R. A. Zalabsky

Citation: J. Chem. Phys. **81**, 5074 (1984); doi: 10.1063/1.447496
View online: http://dx.doi.org/10.1063/1.447496
View Table of Contents: http://jcp.aip.org/resource/1/JCPSA6/v81/i11
Published by the AIP Publishing LLC.

# The homogeneous nucleation of nonane

G. W. Adams[a], J. L. Schmitt, and R. A. Zalabsky
*Physics Department and Graduate Center for Cloud Physics, University of Missouri-Rolla, Rolla, Missouri 65401*

(Received 21 May 1984; accepted 9 July 1984)

The homogeneous nucleation rate of *n*-nonane has been measured as a function of temperature and supersaturation ratio in a precision fast-expansion chamber. The measured nucleation rate ranges from $10^2$ to $10^5$ drops/cm$^3$ over the temperature range 215–270 K. The results have been compared to the classical theory and to the classical theory with the RKC replacement factor. The RKC theory functional form is the basis for an empirical rate equation to fit the data. A full listing of the thermodynamic constants used for the reduction of the data is given.

## I. INTRODUCTION

The homogeneous nucleation of a vapor is the process through which, in the absence of surfaces, aerosol particles and ions, the vapor undergoes dropwise condensation, i.e., the first fragments of the liquid phase appear. Its relative physical simplicity, i.e., it is a system of molecules of only one substance, makes an understanding of homogeneous nucleation fundamental. Such an understanding should provide a firm base upon which to study more complex multicomponent and heterogeneous nucleation.

This paper presents an extensive new data set taken with a precision expansion chamber for the homogeneous nucleation of *n*-nonane. In addition, an empirical equation is given for the calculation of the nucleation rate (drops/cm$^3$ s) over the range of measurements. Finally, the data set is compared to the "classical" theory of Volmer,[1] Becker and Doring,[2] and Zeldovitch,[3,4] and the theory of Reiss, Katz, and Cohen[5] (RKC) and Reiss.[6]

We have recently described our work on ethanol and toluene in papers by Schmitt, Adams, and Zalabsky[7] and Schmitt, Zalabsky, and Adams.[8] These papers detail the experimental techniques used for our expansion chamber measurements of homogeneous vapor to liquid nucleation. They also briefly review the current work in homogeneous nucleation. The expansion chamber used to make the measurements on *n*-nonane is described by Schmitt[9] and further information on expansion chambers is found in Schmitt, Kassner, and Podzimek.[10] Since our measurements on *n*-nonane have been conducted with the same apparatus and the same techniques fully described in the above references, to avoid duplication we have chosen to report only our results for *n*-nonane.

## II. THE DATA SET

Figure 1 shows the measured drop concentrations from the expansion chamber. The curves are a fit to all of our data by the empirical nucleation rate equation (see below). Analyses of drop counts made in this Center over many years for both data analysis and as checks for internal consistency among observers has led to the conclusion that the error associated with the visual drop counts from photographic film is accurately described by the Poisson error distribution. For most data points in Fig. 1 at least 1000 drops were counted on the film and the associated error in the drop count is the square root of the total count. For the case of low drop concentrations, where it is difficult to obtain 1000 counts, a chamber volume of at least 10 cm$^3$ is used as the basis for the reported drop count.

There are several possible, poorly defined, sources of error in the temperature and supersaturation ratio calculations. These include uncertainties in the interaction virial coefficient and saturation vapor pressure of the nonane. Also, the equation of state for the gas mixture is extrapolated into the supersaturated region. More well defined is a maximum error of 0.75% in the supersaturation ratio due to the pressure transducer error ( $\pm$ 0.5 mmHg). Finally a known 0.1 K/cm temperature gradient is introduced into the chamber to produce stability against convection. This of course introduces uncertainty into the temperature and saturation initially present in the sensitive volume of the chamber. Our best estimate of the cumulative error from all of the above considerations places that error in the range of 1% to 2% for supersaturation ratio and for temperature a much smaller error. We estimate that our nucleation rates (drops/cm$^3$s) from our empirical equation (below) are accurate to 50%. We have long recognized the difficulty of plac-

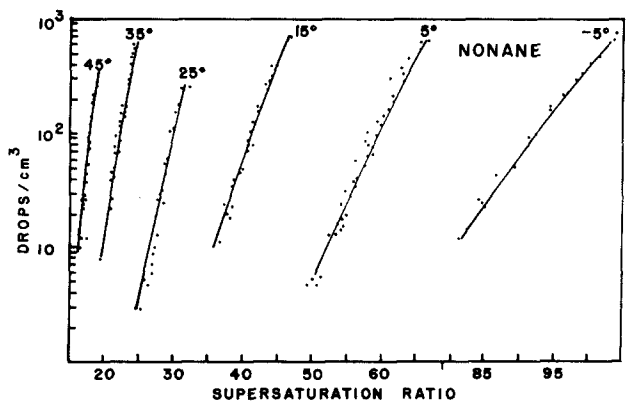


FIG. 1. Measurements of the drops/cm$^3$ (not per s) nucleated in nonane as a function of supersaturation ratio. The solid curves show the empirical fit to the data. The preexpansion temperature of each data group is near the top of the graph.

[a] Now at the Air Purification Section, Chemistry Branch, Chemical Research and Development Center, Aberdeen Proving Ground, MD 21010.

 0021-9606/84/235074-05$02.10 

ing accurate error estimates on our data. We therefore have adopted the policy of making available to other investigators all our nucleation and thermodynamics data (see the Appendix).

## III. COMPARISON WITH THEORY

Two functional forms were enlisted to fit our data. The data first were fitted to an expression for the nucleation rate of the form

$$J(T,S) = S^2 \exp[A(T) + B(T)/(\ln S)^2], \quad (1)$$

where $A(T)$ and $B(T)$ are polynomial functions of temperature $T$ and $S$ is the supersaturation ratio. This form was chosen for comparison with the classical theory

$$J_{\text{class}}(T,S) = S^2 \exp[A_c(T) + B_c(T)/(\ln S)^2]. \quad (2)$$

Here the expressions $A_c(T)$ and $B_c(T)$ are given by

$$A_c(T) = \ln[(\alpha/d)(2\sigma M_w N_0^3/\pi)^{1/2}(P_e/RT)^2] \quad (3)$$

and

$$B_c(T) = -(16N_0 p/3)(M_w/d)^2(\sigma/RT)^3, \quad (4)$$

where $\alpha$ is the sticking coefficient, $d$ is the bulk liquid density, $\sigma$ the bulk surface tension, $P_e$ the saturation vapor pressure, $R$ the gas constant, $N_0$ Avogadro's number, and $M_w$ the molecular weight. Since $\alpha$, $\sigma$, $P_e$, and $d$ are functions only of temperature, $A_c(T)$ and $B_c(T)$ are functions only of temperature and correspond to the $A(T)$ and $B(T)$ functions in Eq. 1.

The second expression chosen incorporates the replacement factor formulated by Reiss, Katz, and Cohen (RKC)[5] and Reiss.[6] It was selected because it produced an excellent fit to our data for toluene (Ref. 8). This second functional form is the classical theory multiplied by the RKC replacement factor

$$J(T,S) = (12/\pi)^{3/2}[-2B(T)/(\ln S)^3]^{1/2} V_g/V_l \times S^2 \exp[A(T) + B(T)/(\ln S)^2], \quad (5)$$

where the first factor is the upper bound of the RKC replacement factor and $V_g$ and $V_l$ are the volume per molecule in the gas and liquid, respectively. As functions of temperature and supersaturation $V_g$ and $V_l$ are

$$V_g = kT/SP_e \quad (6)$$

$$V_l = M_w/N_0 d(T), \quad (7)$$

where $k$ is the Boltzman constant. Again $A(T)$ and $B(T)$ are polynomial functions of temperature in the empirical equation and correspond to $A_c(T)$ and $B_c(T)$ in the classical theory.

For both of the above functional forms coefficients of $A(T)$ and $B(T)$ were determined by a nonlinear least squares search procedure which minimized the quantity

$$\chi^2 = \sum_{i=1}^{N} (1/N_i^m)(N_i^m - N_i^c)^2, \quad (8)$$

where the $N_i^m$ are the measured drop concentrations and $N_i^c$ are those found by integrating the empirical nucleation rate equation over the nucleation pulse. That is,

$$N_i^c = \int_{-t_0}^{+t_0} J[S(t),T(t)]dt. \quad (9)$$

The thermodynamic calculations described above (and in Refs. 7 and 8) generated supersaturation vs time and temperature vs time profiles from the experimental pressure vs time profile ("pulse" profile). The pressure vs time profile has been measured at regular intervals over the course of our experiments. These measurements show no significant change. Practically, the integration limits on the nucleation pulse initially were chosen as $\pm 0.005$ s and increased until no significant changes took place in the functions $A(T)$ and $B(T)$.

The classical and RKC theories are now to be compared on the basis of how well the unaided theory (with a sticking coefficient of 1) predicts our measurements and how well the respective empirical equations resulting from the fit to the measurements predict physically "real" sticking coefficients and surface tensions.

Figure 2 shows the prediction of the classical theory with a sticking coefficient of 1 as compared to our data. To the side of each curve (in bold print) is the factor required to bring the classical theory into the displayed agreement with the data. One sees large factors are required to obtain agreement and a systematic trend from higher to lower temperatures over the range of $10^2$ to $10^9$ in the factors.

Figure 3 shows the predictions of the classical theory multiplied by the RKC replacement factor (again with a sticking coefficient of 1). To the side of each curve (in bold print) is the factor required to bring theory into the displayed agreement. One sees excellent agreement at 15 °C, but large deviations at the extremes—from $3\times10^{-4}$ to $10^2$ (highest to lowest temperature, respectively). However, for both theories the slope of the curves is essentially correct.

By equating $A(T)$ and $B(T)$ in the functional expressions to $A_c(T)$ and $B_c(T)$ [Eqs. (3) and (4)], one can infer the values of the sticking coefficient and the surface tension that would be required to bring the theory into good agreement with data over all temperatures. The results of these calculations are shown in Figs. 4 and 5. Examination clearly shows that the sticking coefficients and surface tensions inferred from the classical theory exhibit nonphysical behavior. However, Fig. 4 shows a well-behaved surface tension inferred from the RKC theory which is about 8% less than the bulk sur-

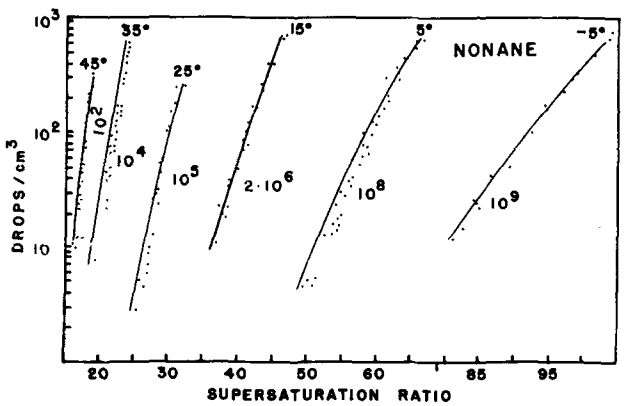


FIG. 2. A comparison of the classical theory to the measurements of nonane nucleation. The solid curves show the classical theory predictions (with a sticking coefficient of 1). Next to each curve is the factor required to bring the prediction into the shown agreement.

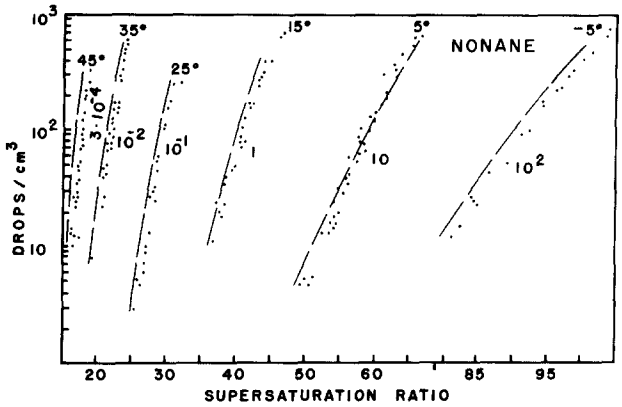


FIG. 3. A comparison of the classical theory multiplied by the RKC replacement factor to the measurements of nonane nucleation. The dashed curves show the theoretical predictions (with a sticking coefficient of 1). Next to each curve is the factor required to bring the prediction into the shown agreement.

face tension and follows the temperature dependence of the bulk. On the other hand, Fig. 5 shows that for the same theory the inferred sticking coefficient, while its functional behavior is better than that for the classical theory, varies from near 1 at 214 K to $10^{-9}$ at 270 K. This latter result implies an extraordinarily long time for the drops in the chamber to grow to visible size; that phenomena is not observed. Also, while experimental measurements for the sticking coefficient as a function of temperature for nonane have not been found in the literature, by analogy with water,[11] one expects it to fall in the range 0.01–1. Because the RKC theory predictions appear closer to physical reality than those of the classical theory, we elected to use it as the basis for the empirical equation to fit the data.

The empirical values for $A(T)$ and $B(T)$ for Eq. (5) are

$$A(T) = -66.683\,827\,7 + 1.128\,489\,287\,92T - 0.338\,165\,341\,878\times10^{-2}T^2 + 0.208\,291\,362\,26\times10^{-5}T^3 \quad (10)$$

and

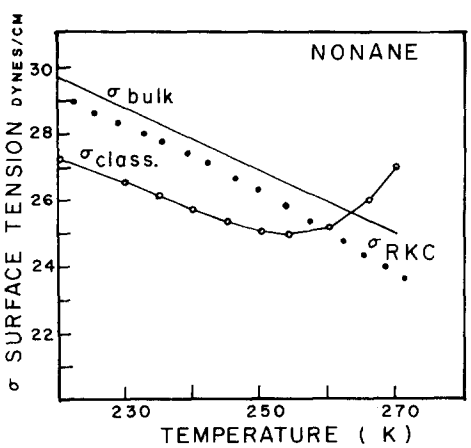


FIG. 4. The surface tension of nonane as a function of temperature as measured and inferred (see the text).

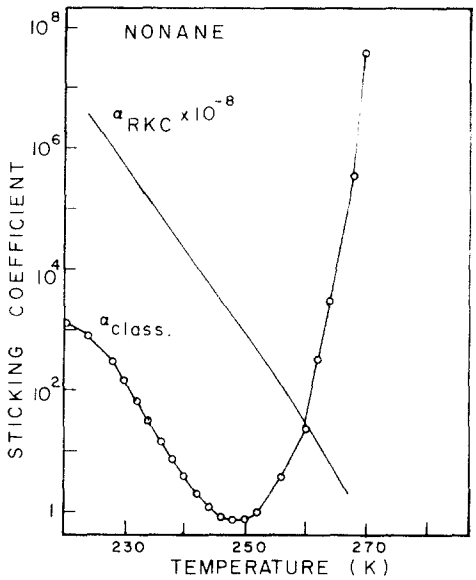


FIG. 5. The sticking coefficient of nonane as predicted by the classical and RKC theories (see the text).

$$B(T) = -3.333\,048\,150\,41\times10^{4} + 3.326\,036\,783\,11\times10^{2}T - 1.136\,796\,238\,06T^2 + 1.323\,811\,521\,86\times10^{-3}T^3. \quad (11)$$

The equation predicts the measured drop counts within 50% over a temperature range of 215–270 K and supersaturation ratio range of 15 to 105. The empirical equation is valid only in this range; this is emphasized since the curve fit has a nonphysical turning point at 312 K which is an artifact of the fitting procedure.

The empirical rate equation can be used for comparison with other $n$-nonane data. However, the only other known published experimental work on $n$-nonane is the critical supersaturation (1 drop/cm$^3$ s) vs temperature measurements of Katz.[12] Katz measured the critical supersaturation with a diffusion cloud chamber and found good agreement with the predictions of the classical theory. Our measurements with the expansion chamber are in the range $10^2$–$10^5$ drops/cm$^3$ s. Thus, to compare our measurements with critical supersaturation measurements it is necessary for us to extrapolate our rate equation two orders of magnitude. Katz' measurements, theoretical predictions, and our (extrapolated) calculated values of critical supersaturation are shown in Fig. 6. The critical supersaturation ratios from our data are closer to the predictions of the RKC theory than to the classical theory. The difference between our values and those of the RKC theory vary from 24% low near 215 K to 16% higher near 270 K with an intersection near 250 K. Our values everywhere are lower than those of Katz (as much as 60% near 240 K). Because our empirical nucleation rate equation must be extrapolated by two orders of magnitude, small errors in the functions $A(T)$ and $B(T)$ could cause large changes in the predicted critical supersaturation ratios. However, such errors do not appear to account for the differences between our calculated values and Katz' measurements.

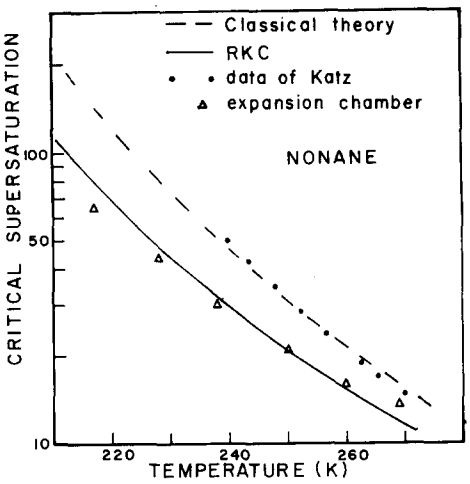


FIG. 6. The critical supersaturation ($J = 1$ drop/cm$^3$ s) as a function of temperature for nonane, as predicted by the classical theory, predicted by the RKC theory, measured by Katz, and predicted by extrapolation of our measurements.

Clearly the nonphysical behavior of the surface tension and sticking coefficient as inferred from the classical theory indicate a missing functional dependence on temperature and supersaturation in that theory. Inclusion of the RKC replacement factor improves the situation, especially in the inferred surface tension, but still does not, as it did in the case of toluene (Ref. 8) produce a physically "real" sticking coefficient. This latter failure may indicate the RKC replacement factor does not adequately compensate for the error introduced by the capillarity approximation (the use of macroscopic parameters such as liquid density, surface tension and sticking coefficient) or it may indicate that the nucleated clusters are not sufficiently large to have properties close to that of the bulk liquid.

The purpose of the experiments described in this article is to provide accurate measurements over a wide range of temperature and supersaturation against which theoretical descriptions of homogeneous nucleation may be tested. The comparison here of our data with theory has shown that a complete theoretical description of homogeneous nucleation has not been developed.

## IV. CONCLUSIONS

We measured the homogeneous nucleation rate for $n$-nonane from $10^2$ to $10^5$ drops/cm$^3$ s over a temperature range of 215–270 K. The measurements were fit to an empirical nucleation rate equation [Eq. (5) with the value of $A(T)$ and $B(T)$ given by Eqs. (10) and (11), respectively] based on the classical theory multiplied by the RKC replacement factor. Various thermodynamic data used for the reduction of the experimental data are given in the Appendix.

The nucleation rates for $n$-nonane are not predicted accurately by the classical nucleation theory which departs from the data increasingly with decreasing temperature. Surface tensions and sticking coefficients inferred from this theory and our data exhibit nonphysical behavior. The inclusion of the RKC replacement factor, which proved quite successful in the case of toluene (Ref. 8), produces considerable improvement in the behavior of the inferred surface tensions, but produces a somewhat nonphysical sticking coefficient. Our analysis suggests that no fully complete theoretical description of homogeneous nucleation has been developed.

## ACKNOWLEDGMENTS

The authors wish to acknowledge the support of the National Science Foundation, Division of Chemical and

TABLE I. Thermodynamic parameters.

Ideal gas heat capacities[a] (erg/mol °K):
$C_{p1} = 5.3664\times10^9\,(0.558\,798 + 1.228\,34\times10^{-3}T - 1.644\,04\times10^{-7}T^2 - 2.465\,34\times10^{-10}T^3)$[b],
$C_{p2} = 2.007\,76\times10^8$.[c]
Saturation vapor pressure for nonane (dyn/cm$^2$):
$P_e(T) = 1332.8947e^x$,
where $x = 20.8468 - 5811.26/T$.[d]
Second virial coefficients (cm$^3$/mol):
$B_1(T) = RT_c/P_c[f^{(0)}(T_r) + \omega f^{(1)}(T_r)]$,[e]
where $T_r = T/T_c$, $T_c = 594.56$ K, $\omega = 0.444\,958$, and
$P_c = 22.58$atm,
$f^{(0)}(T_r) = 0.1445 - 0.330/T_r - 0.1385/T_r^2 - 0.0121/T_r^3$,
$f^{(1)}(T_r) = 0.073 + 0.46/T_r - 0.50/T_r^2 - 0.097/T_r^3 - 0.0073/T_r^8$,
$B_2(T) = -1150.935 + 20.7692T - 0.167\,822\,3\,T^2 + 0.712\,531\,2$
$\times10^{-3}T^3 - 0.154\,184\,1\times10^{-5}T^4 + 0.134\,154\,2\times10^{-8}T^5$.[f]
Liquid density (g/cm$^3$):
$d = 0.7333 - 7.5\times10^{-4}(T - 273.15) + 4.55\times10^{-7}(T - 273.15)^2$.[c]
Surface tension (dyn/cm$^2$):
$\sigma = 24.72 - 0.093\,47(T - 273.15)$.[g]

[a] Subscript 1 refers to the nonane and 2 to the argon.
[b] *Thermophysical Properties of Matter* (IFI/Plenum, New York, 1970), Vol. 6.
[c] Thermodynamics Research Center, *Selected Values of Properties of Hydrocarbons and Related Compounds* (Texas A & M University, College Station, Texas, 1965).
[d] G. F. Carruth and R. Kobayashi, J. Chem. Eng. Data **18**, 115 (1973).
[e] K. S. Pitzer and R. F. Curl, J. Am. Chem. Soc. **79**, 2369 (1957).
[f] From fit of points in *The Thermodynamic Properties of Argon from the Triple Point to 300 K at Pressures to 1000 Atmospheres*, Natl. Bur. Stand. Ref. Data Ser. No. 27 (U. S. GPO, Washington, D. C., 1969).
[g] J. L. Jasper, J. Chem. Ref. Data **1**, 841 (1972).

Process Engineering. B. Smith of Washington University, St. Louis, Missouri has provided references and critically examined thermodynamics data. This work is based upon the Ph. D. dissertation of G. W. Adams.[13]

## APPENDIX

Table I lists the various thermodynamic quantities that were used in the reduction of the data. A list of the data points that are plotted in Figs. 1, 2, and 3 is available upon application to the authors. The data includes the initial (preexpansion) chamber pressure, the minimum (peak) pressure, the calculated expanded temperature, the calculated peak supersaturation ratio, the measured drop count, and the drop count calculated from the empirical fit to Eq. (5). The pressure pulse for all data sets is given by

$$P(t) = P_{\min} + 1.143t + (3.3945 \times 10^5)t^2,$$

where $0.01 > t > -0.01$ s ($t$ is measured from the peak of the pulse), $t$ is in s, and $P$ is in mmHg.

[1]M. Volmer, Z. Phys. Chem. **25**, 555 (1929).
[2]R. Becker and W. Doring, Ann. Phys. (Leipzig) **24**, 719 (1935).
[3]J. B. Zeldovitch, J. Exp. Theor. Phys. **12**, 525 (1942).
[4]J. B. Zeldovitch, Acta. Phys. Chem. **18**, 1 (1943).
[5]H. Reiss, J. L. Katz, and E. R. Cohen, J. Chem. Phys. **48**, 5553 (1968).
[6]H. Reiss, in *Nucleation Phenomena*, edited by A. C. Zettlemoyer (Elsevier, New York, 1977).
[7]J. L. Schmitt, G. W. Adams, and R. A. Zalabsky, J. Chem. Phys. **77**, 2089 (1982).
[8]J. L. Schmitt, R. A. Zalabsky, and G. W. Adams, J. Chem. Phys. **79**, 4496 (1983).
[9]J. L. Schmitt, Rev. Sci. Instrum. **52**, 1749 (1981).
[10]J. L. Schmitt, J. L. Kassner, Jr., and J. Podzimek, J. Aerosol Sci. **13** 373 (1982).
[11]H. R. Pruppacher and J. D. Klett, *Microphysics of Clouds and Precipitation* (Reidel, Boston, 1978), p. 134.
[12]J. L. Katz, J. Chem. Phys. **52**, 4733 (1970).
[13]G. W. Adams, Ph. D. dissertation, University of Missouri-Rolla, Rolla, Missouri, 1983.